Volume 1 | Number 1 | Jan 2013 | Pages 1–100

Journal of
Materials Chemistry B

Materials for biology and medicine
www.rsc.org/materialsB

ROYAL SOCIETY
OF CHEMISTRY

ROYAL SOCIETY
OF CHEMISTRY

www.rsc.org/materialsB

Journal Name

ARTICLE

A pH-responsive natural cyclopeptide RA-V drug formulation for improved breast cancer therapy

Zeng-Ying Qiao,[a,§] Di Zhang,[a,§] Chun-Yuan Hou,[a] Si-Meng Zhao,[b] Ya Liu,[c] Yu-Juan Gao,[a] Ning-Hua Tan,[*,b] and Hao Wang[*,a]

The natural plant cyclopeptide RA-V, which was isolated from the roots of *Rubia yunnanensis*, has been discovered as a novel anti-cancer candidate. However, the cyclic hexapeptide exhibited poor solubility in physiological condition, limiting its application for cancer therapy *in vivo*. To solve this problem, pH-sensitive polymers were developed for targeted RA-V delivery into tumor sites and acid-triggered drug release. The poly(β-amino ester)s (PAE) copolymers self-assembled into micelle-like nanoparticles in aqueous solution at pH 7.4, and the solubility of RA-V was enhanced by loading the drug into hydrophobic cores of micelles. The near-infrared (NIR) fluorescent probe squaraine (SQ) dye as an imaging probe could also be encapsulated into polymer micelles simultaneously. The diameters of RA-V/SQ loaded micelles were measured by dynamic light scattering (DLS) and transmission electron microscopy (TEM), proving that the micelles with sizes of 35-60 nm were suitable as anti-cancer drug nano-vehicles. The drug-loading capacity and drug release profiles of RA-V loaded micelles were calculated and monitored by high performance liquid chromatography (HPLC) measurements. The RA-V/SQ loaded micelles were stable at neutral pH, and drug release could be greatly accelerated by acid-triggered ionization of copolymer chains. Similarly with free RA-V cyclopeptide, the RA-V/SQ loaded micelles exhibit highly anti-cancer efficiency toward MCF-7 cells and Hela cells, while the intact polymer micelles and SQ loaded micelles are non-toxic. Meanwhile, the endocytosis pathway and mitochondria-regulated apoptosis of RA-V/SQ loaded micelles were proved by lysosome colocalization and JC-1 assay, respectively. Finally, biodistribution and tumor growth inhibition were evaluated in MCF-7 cell-xenografted nude mice, demonstrating that RA-V/SQ loaded micelles could realize the tumor imaging and inhibit tumor growth effectively simultaneously. Therefore, the RA-V/SQ loaded micelles may be used as potential nano-scaled cancer therapeutics and imaging agents.

Introduction

As a major public health concern, cancer therapy has attracted much attention in recent years. Researchers have developed various anti-cancer drugs, which have major limitations such as toxicity and chemotherapy resistance in the treatment of patients.[1-3] Therefore, searching new chemotherapeutics, especially plant-derived natural products, plays a vital role in order to realize optimal cancer chemotherapy due to their extensive source from nature.[4, 5] A unique natural cyclopeptide, named as RA-V (deoxybouvardin), is isolated from the medical plant *Rubia yunnanensis* (family Rubiaceae) in Yunnan province of China, which exhibits various pharmacological activities including anti-tumor, anti-inflammatory, and anti-

angiogenesis activities.[6-8] Recently, the anti-tumor mechanisms of RA-V in a variety of cancer cell lines have been reported.[6, 7, 9] However, the current studies of RA-V were limited in cell level due to the poor solubility of RA-V in physiological condition.

In order to apply the cyclopeptide *in vivo*, a pH-sensitive polymer carrier was utilized for loading and controllably releasing RA-V cyclopeptide. The copolymers with hydrophilic and hydrophobic moieties can form nano-scaled aggregates, such as nanogels, nanoparticles, micelles and vesicles, encapsulating hydrophobic molecules in hydrophobic microdomains.[10-15] Polymeric drug nanocarriers have many advantages compared with small drug molecules, which can prolong the blood circulation time, enhance accumulation at

tumor sites via an enhanced permeability and retention (EPR) effect and decrease the systemic toxicity. In view of the weakly acidic environment in the intracellular compartments such as endosomes and lysosomes (pH ~5-6), pH-sensitive polymers have been applied as drug carriers, which are stable in blood circulation and release the loaded drugs in acidic intracellular compartments.[16-20] Polymers with amine groups, acetals/ketals, ortho esters and hydrazine/imide bonds have been reported as pH-sensitive drug nanocarriers.[21-28] Among them, poly(β-amino ester)s containing tertiary amine groups with pK_b at 6.5 have been developed as drug carriers.[29] At physiological pH, the tertiary amine groups are uncharged and hydrophobic, resulting in the formation of polymeric aggregates. As the pH decreases below the pK_b, the aggregates dissociates because the ionization of the tertiary amine causes increased hydrophilicity and electrostatic repulsions of the polymers. PEG modified poly(β-amino ester)s could form nanoparticles loading anticancer drugs and release the loaded cargos at acidic pH, realizing the targeted and controlled drug delivery.[30-35] We have reported poly(RGD-co-β-amino ester) copolymers through the simple, reliable and one-pot synthesis method, which could load and controllably release doxorubicin (DOX), killing U87 cells efficiently.[36] The DOX release behaviors from pH-sensitive poly(β-amino ester)s in cells were also monitored by photoacoustic imaging.[37] Although a large number of pH-sensitive polymers were studied as chemotherapeutic drug carriers, RA-V cyclopeptide loaded polymeric nanoparticles for cancer therapy have not been reported *in vitro* and *in vivo*.

Furthermore, the introduction of imaging agents into nanomedicine plays a vital role on improving the survival of cancer patients, due to the visualization of drug distribution and accumulation at targeted sites non-invasively, the real-time monitoring of the therapeutic responses and so on.[38-45] Near-infrared (NIR) fluorescent dyes, especially squaraine dyes, have been applied for bioimaging due to their high absorption co-efficiency, bright fluorescence and good photostability.[46-49] Würthner *et al* have developed a series of dicyanovinyl-functionalized squaraine (SQ) dyes with superior NIR fluorescence properties and high chemical stability.[46, 50-52] The hydrophobic SQ dyes can be incorporated in BSA and liposomes for tumor imaging *in vivo*.[53-56]

Herein, we synthesized PEG grafted poly(β-amino ester)s through the simple and facile Michael-type addition, which could self-assemble into micelle-like nanoparticles at neutral pH. Natural cyclopeptide RA-V and NIR fluorescent probe SQ were loaded into hydrophobic cores of polymeric micelles with diameter below 100 nm and high stability (Scheme 1). The micelles delivered RA-V cyclopeptide and SQ into cancer cells by cellular endocytosis efficiently, which were proved by monitoring SQ fluorescent signals. The anti-cancer efficiency of RA-V/SQ loaded micelles toward Hela and MCF-7 cells were comparable with that of free cyclopeptide. The cell apoptosis was related with mitochondria disruption, resulting in strong anti-tumor activity against cancer cells. The *in vivo* imaging experiment demonstrated that RA-V/SQ loaded micelles accumulated the targeted tumor sites by EPR effect.

Furthermore, the RA-V/SQ loaded micelles were injected into MCF-7 tumor-bearing nude mice through the tail vein, exhibiting effective tumor suppression activity. Therefore, the RA-V/SQ loaded PAE micelles are promising candidates as effective anti-tumor nano-sized theranostic agents.
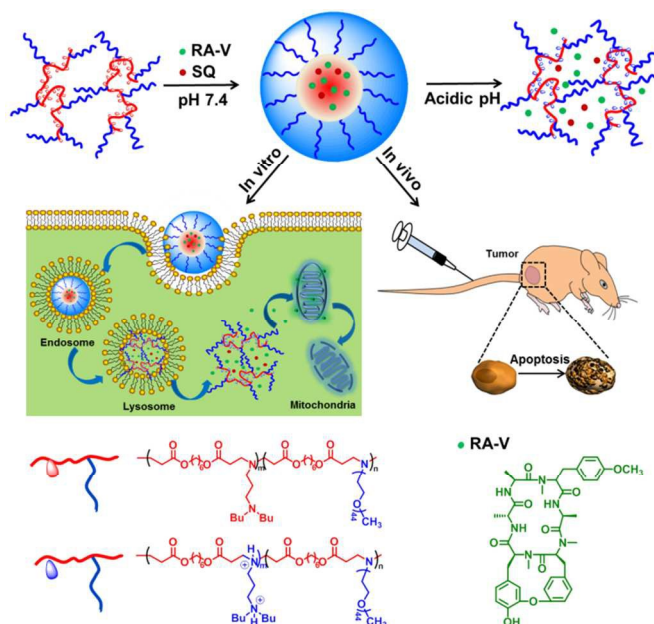
Scheme 1. The co-encapsulation of RA-V cyclopeptide and SQ molecules in pH-sensitive PAE micelles for efficient tumor therapy and imaging *in vitro* and *in vivo*.

Materials and methods

Materials

RA-V (>99%) was isolated from *R. yunnanensis* as described before.[7] RA-V was dissolved in DMSO (20 mM) as a stock solution, stored at -18 °C, and diluted with medium for each experiment. 3-(Dibutylamino)-1-propylamine (DBPA), and 1,6-Hexanediol diacrylate (HDDA) were purchased from Aldrich-Sigma Chemical Corporation. Methyl PEG-NH$_2$ 2K (Seebio Biotech, Inc.), cell counting kit-8 assay (CCK-8, Beyotime Institute of Biothechnology, China), JC-1 assay kit and LysoTracker Green DND-26 (Invitrogen Co.) were used without further purification. MCF-7 and Hela cell line were purchased from cell culture center of Institute of Basic Medical Sciences, Chinese Academy of Medical Sciences (Beijing, China). Other solvents and reagents were used as received.

Preparation of RA-V/SQ loaded copolymer micelles

The RA-V/SQ loaded copolymer micelles were prepared using the dialysis method. Take the RA-V/SQ-loading experiment (Table 1, Run 4) as an example. PAE copolymers (6.0 mg), RA-V (0.6 mg) and SQ (180 μM) were first dissolved in DMSO (1.0 mL). 2 mL PB (10 mM, pH 7.4) was added dropwisely (50 μL/min) under constantly stirring. The resultant solution was then dialyzed against PB (pH = 7.4) for 24 h (MWCO: 2000 Da) in dark to form the RA-V/SQ-loaded

micelles, and the dispersion volume was finally set to 6 mL (1.0 mg/mL for PAE and 30 μM for SQ). All the measurements were performed in triplicate in the dark. For calculation of the RA-V loading capacity and efficiency, the micelles were dissolved by adding acetonitrile. The calibration curve was obtained by a series of solutions with various RA-V concentrations on a Waters 2796 HPLC. The solutions were passed through syringe filters (0.22 μm) before measurements. For HPLC measurements, the sample solution was injected through a 20 μL sample loop, and a mixture of acetonitrile/water (v/v=45/55) was used as the mobile phase at a flow rate of 1.0 mL/min. The column temperature was maintained at 25 °C, and the column effluent was detected at 220 nm by a UV detector. The loading capacity (LC) and loading efficiency (LE) was defined as RA-V in PAE micelles/PAE micelles (wt%) and RA-V in PAE micelles/RA-V in feed (wt%), respectively.

UV-Vis absorption and fluorescence spectra

In order to measure the UV spectra of SQ in polymer micelles, we first prepared the SQ-loaded micelles as above mentioned. The absorption spectra of free SQ (30 μM, 10mM PB with 1% DMSO) and SQ-loaded PAE micelles (1.0 mg/mL for PAE and 30 μM for SQ in 10 mM PB, pH 7.4) were measured on a Shimadzu UV-2600 spectrometer. The fluorescent emission spectra of free SQ and SQ-loaded copolymer micelles were measured on an F-280 fluorometer with the excitation wavelength of 705 nm. The fluorescence intensity from 720 nm to 780 nm was recorded.

pH-dependent RA-V release profiles

The release profiles of RA-V from the micelles were obtained in the PB solutions (pH 7.4 and pH 5.0). The absorption of the RA-V loaded micelles（1 mg/mL）was first measured on a Waters 2796 HPLC at 220 nm as 0 time point. Then the micelles were passed through syringe filters (0.22 μm), and the HPLC absorptions of the filtrate were recorded at specific time points. Percent cumulative release of RA-V was calculated according to the formula $(A_0-A)/A_0 \times 100\%$, where A_0 and A denote the absorbance peak area at 0 time point and a specific incubation time point, respectively.

Cell growth inhibition assay for MCF-7 and Hela cells

MCF-7 cells were used to evaluate the anti-cancer effect of RA-V/SQ loaded micelles by the CCK-8 assay. Free RA-V, PAE micelles, SQ-loaded micelles, RA-V/SQ loaded micelles were dispersed in PBS (10 mM, pH 7.4) with a series of different concentrations. A density of 5×10^3 cells per well were seeded in the 96-well plates in DMEM containing 10% FBS and 1% penicillin-streptomycin in a humidified atmosphere with 5% CO_2 and then cultured at 37 °C for 24 h. 10 μL of the sample solutions with different concentrations were added to each well, and the cells were incubated for additional 24 h or 72 h, followed by washing with PBS twice. Then 10 μL of CCK-8 solutions was added to each well and cultured for another 4 h. The UV-Vis absorptions of sample wells (A_{sample}) and control

wells ($A_{control}$) were measured using a Microplate reader at a test wavelength of 450 nm and a reference wavelength of 690 nm, respectively. Cell viability (%) was equal to ($A_{sample}/A_{control}$) *100. All the experiments were performed in triplicate. The cell growth inhibition assay for Hela cells were performed with the similar procedures.

Confocal laser scanning microscopy (CLSM) observation

MCF-7 cells were cultured in complete DMEM at 37 °C in a humidified atmosphere containing 5% CO_2 for 24 h. MCF-7 cells were first treated with free SQ (3 μM) and SQ-loaded PAE micelles (100 μg/mL for micelles and 3 μM for SQ) for 2 h and then washed with PBS three times. The cells were incubated with LysoTracker Green DND-26 (10 mM) for 30 minutes, and then washed with PBS three times. After replacement of medium, cells were imaged using a Zeiss LSM710 confocal laser scanning microscope with a 63× objective lens.

Mitochondria-regulated apoptosis by JC-1 assay

MCF-7 cells were cultured as above mentioned. For JC-1 assay, free RA-V (0.38 μg/mL，500 nM), PAE micelles (7.56 μg/mL) and RA-V loaded micelles (7.94 μg/mL) were dispersed in DMEM media (2 mL), which were added into cells grown in a confocal microscope dish. The cells were further incubated at 37 °C in a humidified atmosphere containing 5% CO_2 for 6 h. The mitochondria were stained with JC-1 in DMEM medium for another 20 min. After removing the medium and washing with PBS, cells were imaged by a spinning disk confocal microscopy (SDCM) observation (UltraVIEW VoX SDSM, PE Co.) with a 63× objective lens.

In vivo imaging of micelles

All animal experiments were performed complying with the National Institutes of Health (NIH) guidelines for the care and use of laboratory animals of Peking University Animal Study Committee's requirements and according to the protocol approved by the Institutional Animal Care. The MCF-7 cells (5 × 10^6 cells) collected in 1640 medium (200 μL) were subcutaneously injected into the rear of 8-week female BALB/c nude mice. Caliper were used to measure tumor size, and the tumor volume was calculated by equation $V=AB^2/2$, where A and B was the maximum and minimum diameters of tumors, respectively. All the tests were performed in quadruplicate. When the transplanted tumor volume reached ~500 mm^3, 200 μL 1 mg/mL RA-V/SQ loaded micelle suspension was injected through a tail vein. After 4 h, the mice were anesthetized and placed in the chamber of an *in vivo* imaging system (CRI Maestro 2), acquiring the whole body images. Mice treated with intravascular injection PBS acted as control group. Then mice were killed and the tumor, heart, liver, spleen, lung and kidney were excised for fluorescent measurement. All images were analyzed and collected with a Maestra *in vivo* imaging system (excitation filter, 705 nm; emission filter, 740 nm).

In vivo antitumor activity

The MCF-7 cells (5×10^6 cells) were transplanted subcutaneously into the rear of 8-week female BALB/c nude mice. When the tumors reached sizes of ~100 mm^3 (14 days after tumor cell implantation), the mice were divided into four groups (N=6) and treated via the tail vein by PBS, PAE micelles, RA-V/SQ loaded control micelles (Pluronic® F-127) and RA-V/SQ loaded PAE micelles (200 μL, ~1 mg/kg for RA-V). The drug was intravenously administered to mice twice every week. During the process of the treatment, the tumor volumes and body weight were evaluated every other day. The tumor inhibition ratio (IR) was calculated by the equation: IR% = $(V_0 - V)/V_0 \times 100\%$, where V_0 was the average tumor volume of control group after treatment with PBS for 15 days, and the V was the average tumor volumes of treatments with PAE micelles, RA-V/SQ loaded control micelles and RA-V/SQ loaded PAE micelles, respectively.

Statistical Analysis

Data are presented as the mean ± standard deviation (SD). Comparison between groups was analysis with the two-tailed Student's t-test. Differences were considered statistically significant when the p values were less than 0.05 ($p < 0.05$). The level of significance was defined at *$p < 0.05$, **$p < 0.01$ and ***$p < 0.001$.

Results and discussion

Formation of RA-V/SQ loaded PAE micelles

Both therapeutic cyclopeptide RA-V and NIR probe SQ were hydrophobic, which limited their application in tumor therapy and imaging. Therefore, the induction of nanovehicles into this system was important for development of novel nanomaterials for tumor diagnosis and treatment. The graft poly(amino ester)s (PAE) copolymers were synthesized by Michael addition (Scheme S1 and Fig. S1), which self-assembled into micelle-like nanoparticles of ~31 nm in aqueous solution at pH 7.4. The hydrophobic RA-V and SQ (Scheme S2) were loaded into PAE micelles with hydrodynamic diameters of 35-60 nm, indicating the stable and effective encapsulation of guest molecules (Fig. 1 and Table 1). The size increase of RA-V/SQ loaded micelle can be attributed to the hydrophobicity of RA-V and SQ, inducing further aggregation of polymer chains. TEM images showed RA-V/SQ loaded micelles were almost spherical, similarly with the blank micelles, and the size increase of micelles was in accordance with the results of DLS (Fig. 2). RA-V was encapsulated into PAE micelles physically, and the loading content and efficiency were determined by HPLC (Fig. S2). As shown in Table 1, the loading content of RA-V/SQ loaded micelles was similar with RA-V loaded micelles, showing that the participation of SQ had no obvious influence on the encapsulation ability of RA-V.

The effective loading of SQ into PAE micelles were verified by UV-Vis and fluorescence spectra (Fig. 3). The absorptions maxima at ~705 nm and ~650 nm corresponded

with the monomer and *H*-aggregate bands, respectively. Compared with free SQ, the absorption of ~705 nm for SQ loaded micelles was enhanced, proving that SQ was encapsulated into micelles mainly as monomer. The red-shift absorption of SQ was benefit for imaging *in vivo*, due to the deeper penetration ability of 705 nm. At excitation wavelength of 705 nm, the fluorescence spectra of SQ loaded micelles and free SQ were measured, indicating that the loaded SQ could emit fluorescence at ~741 nm with high intensity, while free SQ could not. Therefore, the SQ loaded PAE micelles could be applied as potential tumor diagnosis agents.
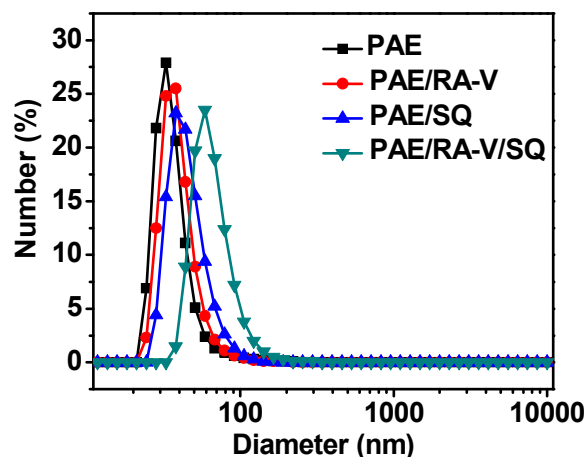

Fig. 1. Number size distribution of PAE micelles, RA-V loaded PAE micelles, SQ loaded PAE micelles, and RA-V/SQ loaded PAE micelles (1.0 mg/mL) in 10 mM PB solutions (pH 7.4) measured by DLS.

Table 1. Properties of RA-V/SQ loaded PAE micelles

Sample	D_{h1} (nm)^a	D_{h2} (nm)^b	D_{h3} (nm)^c	w_d/w_p (wt%)^d	LC (wt%)^e	LE (wt%)^f
PAE	31.2	8.5	32.3	N/A	N/A	N/A
PAE/RA-V	35.6	174.2	34.8	10	5.64	56.4
PAE/SQ	41.5	10.8	43.6	N/A	N/A	N/A
PAE/RA-V/SQ	59.2	169.5	57.6	10	5.82	58.2

^{a} Average hydrodynamic diameter and dispersity index measured by DLS for the copolymer micelle dispersions (pH 7.4, 10 mM PB). ^{b} Average hydrodynamic diameter measured by DLS for the copolymer micelle dispersions (pH 5.0, 50 mM acetate buffer solution). ^{c} Average hydrodynamic diameter measured by DLS for the copolymer micelle dispersions (pH 7.4, 10 mM PB) after 24 h. ^{d} w_d/w_p denotes the initial RA-V/polymer ratio in feed. ^{e} Loading capacity (LC) is defined as the percent ratio of RA-V in PAE micelles/PAE micelles. ^{f} Loading efficiency (LE) is defined as the percent ratio of RA-V in PAE micelles/ RA-V in feed.
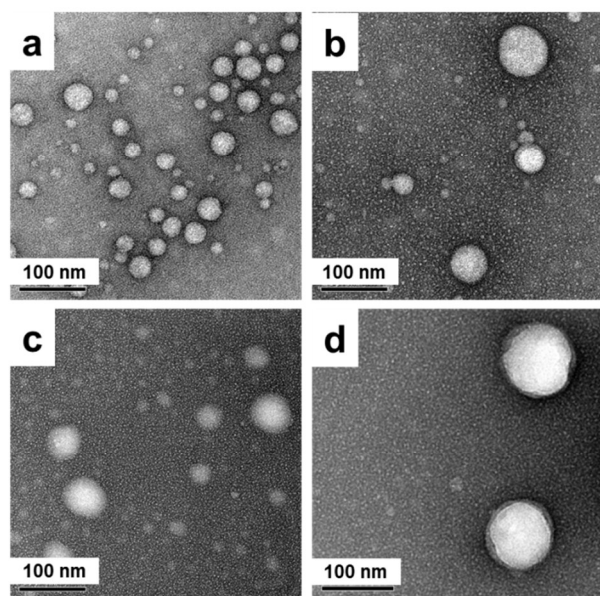
Fig. 2. TEM images of (a) PAE micelles, (b) RA-V loaded PAE micelles, (c) SQ loaded PAE micelles and (d) RA-V/SQ loaded PAE micelles (1.0 mg/mL) in 10 mM PB solutions at pH 7.4.
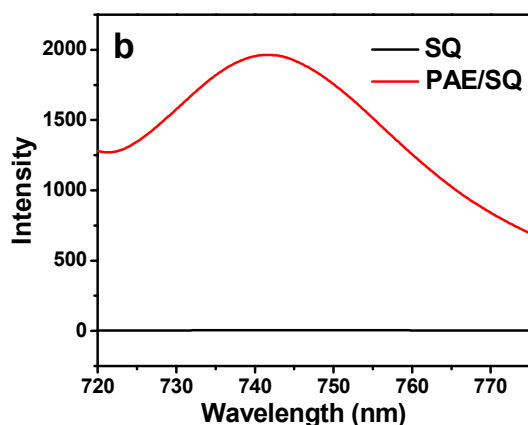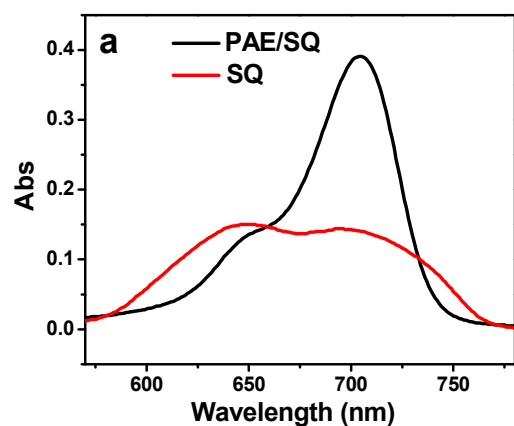

Fig. 3. (a) UV-Vis absorption spectra of SQ loaded PAE micelles (1 mg/mL) in 10 mM PB solutions at pH 7.4 and free SQ in 10 mM PB solutions containing 1% DMSO. (b) Florescence emission spectra of SQ loaded PAE micelles (1 mg/mL) in 10 mM PB solutions at pH 7.4 and free SQ in 10 mM PB solutions containing 1% DMSO. λ_{ex}=705 nm. SQ concentration: 30 µM.

Acid-triggered RA-V release from PAE micelles

As we know, the acidic media could induce the protonation of tertiary amines of PAE, followed by the dissociation of polymer chains below 10 nm. However, when hydrophobic guest molecules were loaded into micelles, the dissociation behavior might change. As shown in Fig. 4a, for RA-V loaded micelles, the larger nanoparticles around 170 nm were measured by DLS at pH 5.0, implying the possible further aggregation of RA-V after release from micelles. It is reasonable that the hydrophobic RA-V were prone to aggregate due to the disappearance of hydrophobic microdomains at acidic condition. The aggregates were not stable enough that larger aggregate formed, which could be filtrated from the micelle dispersion. The RA-V release profiles were monitored at different pHs (Fig. 4b), and filtration at specific time point was executed for calculating the released RA-V that was quantified by HPLC. At pH 7.4, only ~20% of the loaded RA-V was released in 5 h, suggesting a satisfactory stability of the RA-V/SQ loaded micelles at physiological condition. In mildly acidic condition (pH 5), the release of RA-V was significantly accelerated, which was attributed to the ionization of tertiary amine groups and the subsequent dissociation of micelles. ~60% and ~86% of RA-V was released from micelles in 50 min and 5 h, respectively, indicating that RA-V could be released after the micelles entered lysosomes, which was vital for exerting the therapeutic effect on cancer cells.

In order to verify that the micelles were suitable for intravenous injection, the stability of the RA-V/SQ loaded micelles in pH 7.4 PBS solutions was evaluated by DLS (Fig. 4c). After incubation of the RA-V/SQ loaded micelles for 7 day, there was no obvious change of diameters of RA-V/SQ loaded micelles, proving the good incubation stability of the RA-V/SQ loaded micelles. Therefore, the RA-V/SQ loaded micelles can be applied as potential nanodrugs for systemic administration.
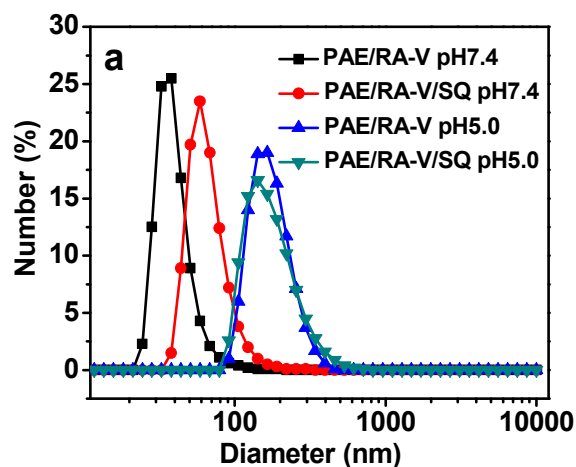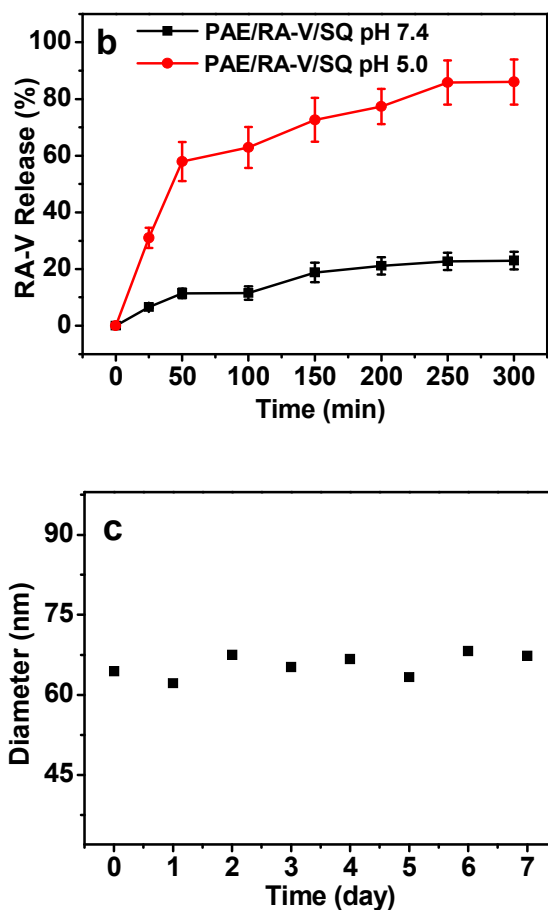
Fig. 4. (a) Number size distribution of RA-V loaded PAE micelles and RA-V/SQ loaded micelles (1.0 mg/mL) in 10 mM PB solutions (pH 7.4) and 50 mM acetate buffer (pH 5.0) measured by DLS. (b) *In vitro* cumulative release profiles of RA-V from RA-V/SQ loaded PAE micelles at pH 7.4 and pH 5.0. (c) Hydrodynamic diameter vs time plots of RA-V/SQ loaded PAE micelles in PBS solution (pH 7.4) at 37 °C. Micelle concentration: 1.0 mg/mL.

In vitro anti-cancer effect of RA-V/SQ loaded micelles

The cyclopeptide RA-V has broad anti-tumor ability in various cancer cell lines, and Hela and MCF-7 cells were used for evaluating the anti-cancer efficiency of drug loaded micelles. The free cyclopeptide and RA-V/SQ loaded micelles both suppressed the growth of Hela and MCF-7 cells in a dose-dependent manner with IC_{50} value of ~5 nM, indicating the effective anti-cancer ability (Fig. 5). For cancer treatment, nanodrugs usually showed lower efficiency of killing cancer cell due to the inefficient cellular internalization of the micelles shielded by the hydrophilic PEG chains.[21, 55, 57] In this nanosystem, the drug loaded micelles exhibit similar cell viability with that of free drug at the same concentration. We speculated that the encapsulation increased the solubility of RA-V facilitating the entrance into cells. Meanwhile, the low IC_{50} value of RA-V could decrease the amount of polymeric carriers, because RA-V with low concentration was enough for killing cancer cells. As the concentration of RA-V increased to 500 nM, PAE micelles and SQ loaded micelles did not display

obvious cytotoxicity. Therefore, the RA-V/SQ loaded micelles could be applied as efficient anti-cancer nanodrugs.
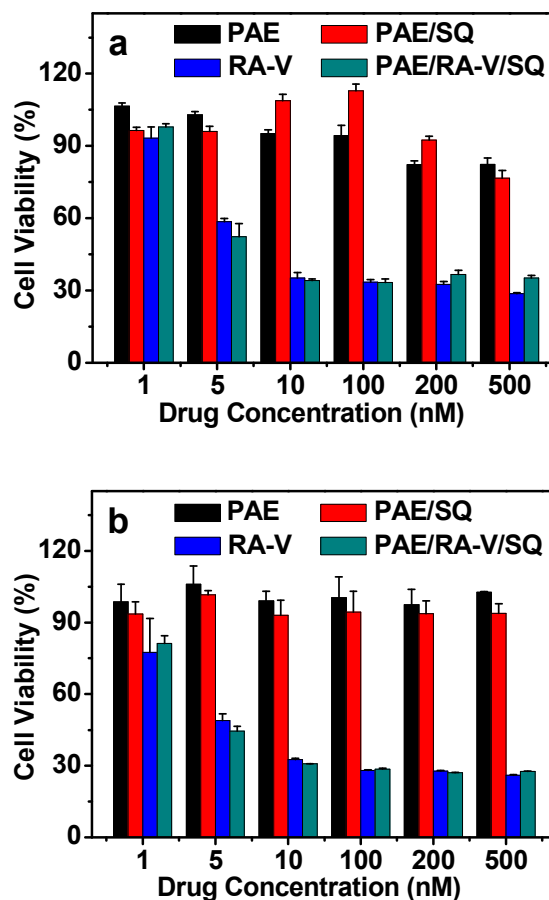

Fig. 5. (a) Hela cell viability and (b) MCF-7 cell viability measured by CCK-8 assay. The RA-V loaded PAE micelles (run 2 in Table 1) with the initial feed ratio of 10% were used for the experiments. Results are presented as the mean ± SD in triplicate.

In vitro anti-cancer mechanism of RA-V/SQ loaded micelles

The cellular internalization process of free RA-V cyclopeptide could not be monitored due to the lack of modification sites in the chemical structures. However, the encapsulation of RA-V into micelles realized the observation of RA-V traffic process. NIR probe SQ and RA-V were loaded into PAE micelles simultaneously, so the cell uptake processes of loaded RA-V could be monitored by SQ fluorescence signal. As shown in Fig. 6, little free SQ entered into cells efficiently in 1 h due to the low solubility of SQ in cell culture media. In contrast, RA-V/SQ loaded micelles could enter into cells by endocytosis pathway in 1 h, proved by the colocalization of micelles and lysosomes. After entrance into cells, the RA-V loaded micelles induced cell apoptosis, which was studied by JC-1 assay (Fig. 7). For PAE micelles, similarly with the control cells without any treatment, red fluorescence signal was observed due to the aggregation of JC-1 monomer into the normal mitochondria forming *J*-aggregate. However, after culturing with RA-V and RA-V loaded micelles, the red fluorescence nearly disappeared

and green fluorescence of *J*-monomer increased indicating mitochondria were destroyed seriously. The results illustrated that RA-V loaded micelles induced cell apoptosis by destroying mitochondria, while PAE micelles did not exhibit obvious cytotoxicity. Therefore, The RA-V/SQ loaded micelles entered cells by endocytosis pathway and released the loaded RA-V in lysosomes acting as a pH trigger. The intracellular release of RA-V induced effective disruption of mitochondria membrane resulting in the high anti-tumor activity.
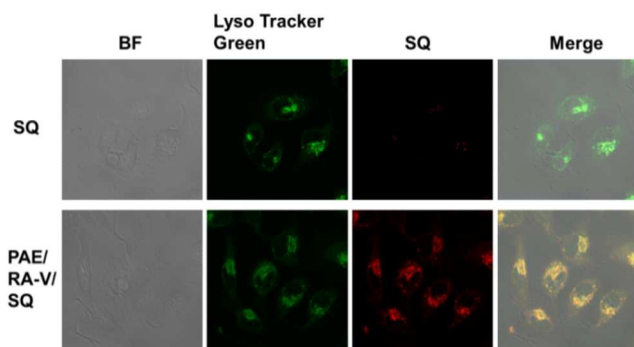

Fig. 6. CLSM microscopy of living MCF-7 cells that were incubated with SQ and RA-V/SQ loaded PAE micelles for 2 h. SQ concentration: 3 μM. Lysosomes were labeled with LysoTracker Green DND-26 for 30 min before imaging.
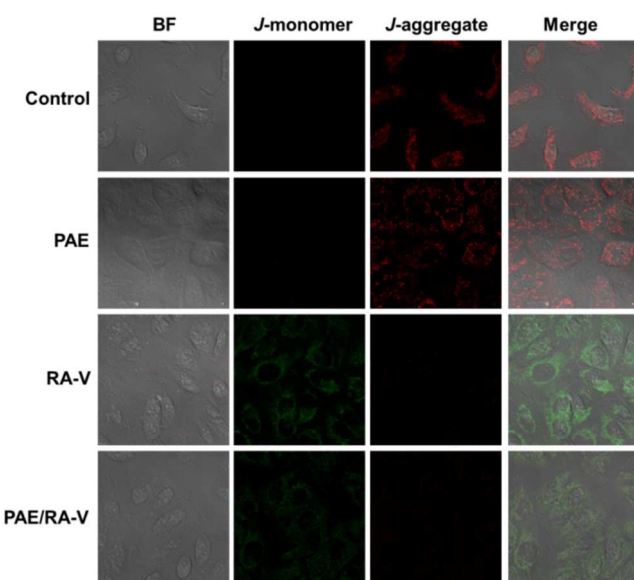

Fig. 7. Comparison of mitochondrial membrane potentials (JC-1 assay) in MCF-7 cells after incubation with PAE micelles, RA-V cyclopeptide and RA-V loaded micelles for 6 h with RA-V concentration at 500 nM.

In vivo tumor imaging.

The aforementioned results suggested that SQ loaded micelles displayed a maximum absorption peak at 705 nm and a fluorescent emission peak at 741 nm, which could enter into cells with high fluorescence intensity. Therefore, the biodistribution of RA-V/SQ loaded micelles were investigated *in vivo* by monitoring the fluorescence signal distribution. RA-V/SQ loaded micelles (200 μL with concentration of 2 mg/mL) were intravenously injected into a nude mouse bearing a

subcutaneous MCF-7 cell-derived xenograft tumor. Mice treated with intravenous injection of PBS were used as control. The optical images of mice were measured after 4 h administration by device camera (Fig. 8a). Strong fluorescent signals around tumor were observed, which were distinguishable from around tissues in the mice, indicating the highly specific tumor targeting ability of micelles by EPR effect. Furthermore, the *ex vivo* experiments were carried out to study the biodistribution of micelles (Fig. 8b). By quantifying the biodistribution of fluorescence intensities of organs, the tumor showed higher signal than other harvested organs, i.e., spleen, lung, heart and kidney (Fig. 8c). The high tumor accumulation of RA-V/SQ loaded micelles and acid-triggered release of drugs resulted in the higher concentration of RA-V in tumor sites, implying the enhanced therapeutic efficacy *in vivo*.
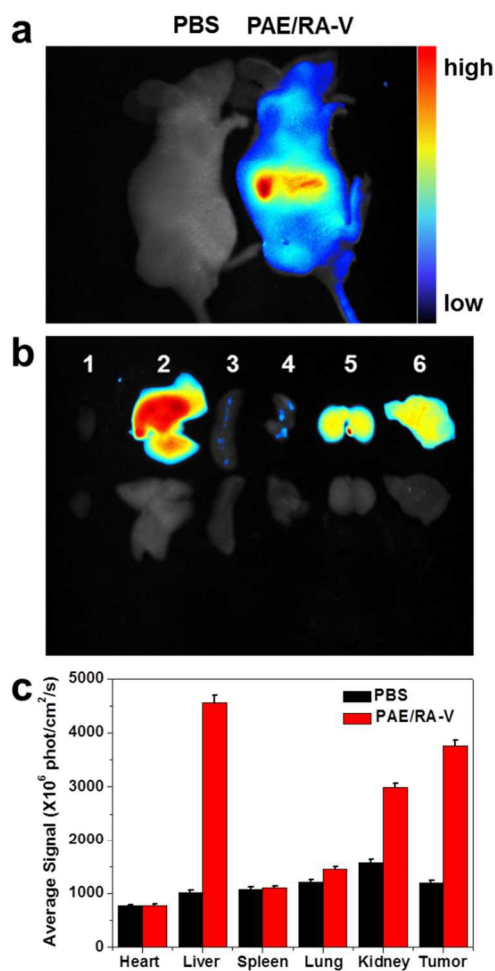

Fig. 8. (a) *In vivo* NIR optical imaging of nude mice bearing MCF-7 tumors 4 h post tail-vein injection of RA-V/SQ loaded PAE micelles (right). Mice treated with PBS were regarded as the control group (left). (b) *Ex vivo* NIR optical imaging of tissues and tumors at 4 h after intravenous administration of RA-V/SQ loaded PAE micelles (above) or PBS (below); 1. Heart; 2. Liver; 3. Spleen; 4. Lung; 5. Kidney; 6. Tumor. (c) Quantitative analysis for the biodistribution of RA-V/SQ loaded PAE micelles in major organs 4 h post-injection to mice. Mice treated with PBS were regarded as the control group. Each column represented the mean value (n=3). Data were represented as means ±S.D.

In vivo anti-tumor effect of micelles.

In vivo tumor suppression studies were executed to investigate the anticancer ability and systemic toxicity of RA-V/SQ loaded micelles using MCF-7 cells xenografted tumor nude mice model. After the tumors were developed to around 100 mm³, we divided the mice into four groups (N = 6) to minimize weight and tumor size differences for studying their comparative efficacy. The process of tumor growth was observed for 15 days, and tumor inhibition efficacy of different groups, i.e., PBS, PAE micelles, RA-V/SQ loaded control micelles and RA-V/SQ loaded PAE micelles were summarized as plots of tumor volumes over the treatment time (Fig. 9a). The free RA-V could not be utilized as control group, because the hydrophobic RA-V would precipitate in aqueous solution and block the blood vein of mice. Pluronic® F-127 was used as control polymer that could form control micelles loading RA-V and SQ with diameter of ~170 nm, since PEO-PPO-PEO block copolymer was widely applied as drug carriers.[58-60] The tumors treated with RA-V/SQ loaded control micelles (inhibition ratio of ~58%) and RA-V/SQ loaded PAE micelles (inhibition ratio of ~71%) increased more slowly than that of PAE micelles (inhibition ratio of ~12%), exhibiting effective anti-tumor ability (Fig. 9b). It was reasonable that nano-scaled RA-V/SQ loaded micelles could accumulate into the tumor site specifically by EPR effect, and RA-V was controllably released in cancer cells. Furthermore, RA-V/SQ loaded PAE micelles with inhibition ratio of ~71% could suppress the tumor growth more significantly than RA-V/SQ loaded control micelles with inhibition ratio of ~58%. We speculated that the smaller size and acid-triggered release behavior of RA-V/SQ loaded PAE micelles might facilitate the specific accumulation and controlled release of RA-V in tumor sites.[61, 62] For most of chemotherapeutics, the injection amount of 5~10 mg/kg was usually used for tumor treatment. In this nanosystem, only 1 mg/kg of RA-V was administered, proving the high anticancer efficiency. The body weight of the mice treated with RA-V/SQ loaded control micelles and RA-V/SQ loaded PAE micelles revealed nearly stable weight between 20 g to 23 g (Fig. 9c), indicating less toxicity of encapsulated RA-V. Therefore, the *in vivo* experiment demonstrated that RA-V/SQ loaded PAE micelles could accumulate into the solid tumor, which resulted in the limited systemic toxicity. The acidic environment in the lysosomes could trigger the release of RA-V and perform enhanced anti-tumor efficiency.
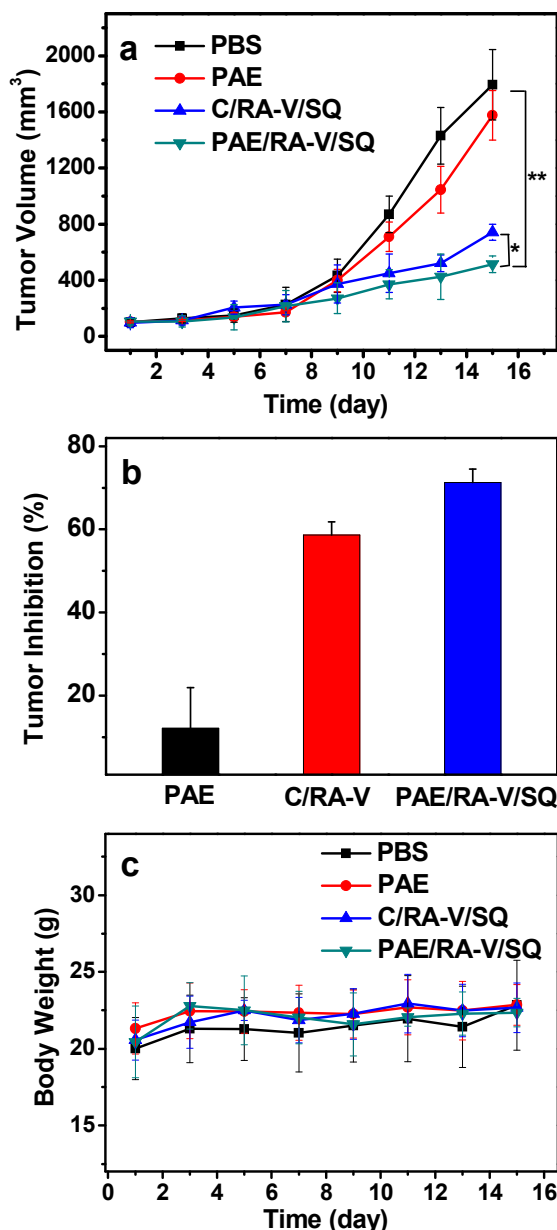
Fig. 9. (a) Tumor volume changes after intravenous injection of PBS, PAE micelles, RA-V loaded control micelles, RA-V loaded PAE micelles in MCF-7 tumor-bearing nude mice. (b) Tumor inhibition ratio in mice after 15 days of different treatments. (c) Body weight changes of the four groups over the course of treatments. Values were expressed as means ±S.D. (N=5). Asterisks (*) denoted statistical significance; Statistical significance: *p <0.05, **p< 0.01 and ***p < 0.001.

Conclusion

We demonstrated the preparation of RA-V/SQ loaded pH-sensitive polymeric micelles for efficient anti-tumor therapy and targeted tumor imaging. Natural cyclopeptide RA-V and NIR fluorescent probe SQ were incorporated into PAE micelles, which could be controllably released in weakly acidic environment. RA-V/SQ loaded micelles could enter cells by endocytosis pathway, release the loaded RA-V and disrupt mitochondria in cells effectively, causing the high anti-cancer

activity. *In vivo* tumor-targeted fluorescence real-time imaging confirmed that RA-V/SQ loaded micelles could be specifically targeted to and retained in the tumor site by EPR effect in nude mice bearing subcutaneous MCF-7 tumors. Importantly, the *in vivo* tumor inhibition ability of RA-V/SQ loaded PAE micelles was higher than that of RA-V/SQ loaded control micelles. Therefore, PAE micelles could effectively deliver RA-V and SQ to tumors for enhanced tumor treatment and imaging. We envision that RA-V/SQ loaded micelles can be applied as potential nano-scaled theranostic agents in the further.

Acknowledgments

Notes and references

[a] CAS Key Laboratory for Biological Effects of Nanomaterials and Nanosafety, National Center for Nanoscience and Technology (NCNST), Beijing, 100190, China.
[b] State Key Laboratory of Phytochemistry and Plant Resources in West China, Kunming Institute of Botany, Chinese Academy of Sciences, Kunming 650201, Yunnan, China.
[c] College of Marine Life Science, Ocean University of China, No. 5 Yushan Road, Qingdao, China.
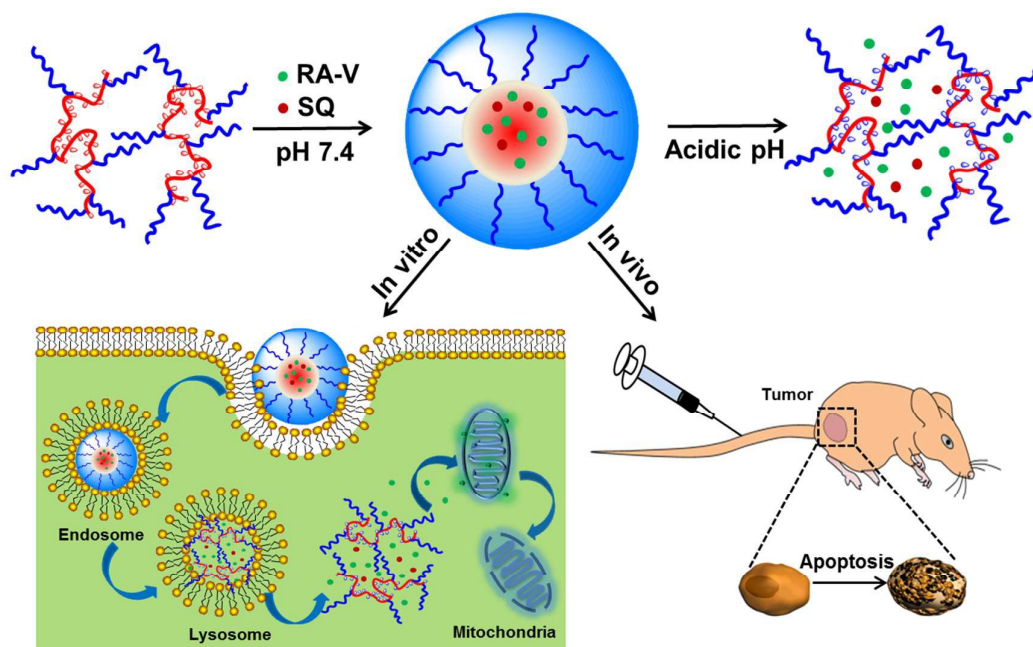§ These authors contributed equally to this work.
Corresponding author: wanghao@nanoctr.cn, nhtan@mail.kib.ac.cn

References

1. L. A. Gilbert and M. T. Hemann, *Cancer Res.*, 2011, **71**, 5062-5066.
2. M. Dean, T. Fojo and S. Bates, *Nat. Rev. Cancer*, 2005, **5**, 275-284.
3. C. Holohan, S. Van Schaeybroeck, D. B. Longley and P. G. Johnston, *Nat. Rev. Cancer*, 2013, **13**, 714-726.
4. N. H. Tan and J. Zhou, *Chem. Rev.*, 2006, **106**, 840-895.
5. J. W. H. Li and J. C. Vederas, *Science*, 2009, **325**, 161-165.
6. J. T. Fan, J. Su, Y. M. Peng, Y. Li, J. Li, Y. B. Zhou, G. Z. Zeng, H. Yan and N. H. Tan, *Biorg. Med. Chem.*, 2010, **18**, 8226-8234.
7. G. G. Yue, J. T. Fan, J. K. Lee, G. Z. Zeng, T. W. Ho, K. P. Fung, P. C. Leung, N. H. Tan and C. B. Lau, *Br. J. Pharmacol.*, 2011, **164**, 1883-1898.
8. H. Itokawa, K. Takeya, N. Mori, T. Hamanaka, T. Sonobe and K. Mihara, *Chem. Pharm. Bull. (Tokyo)*, 1984, **32**, 284-290.
9. X. Y. Fang, W. Chen, J. T. Fan, R. Song, L. Wang, Y. H. Gu, G. Z. Zeng, Y. Shen, X. F. Wu, N. H. Tan, Q. Xu and Y. Sun, *Toxicol. Appl. Pharmacol.*, 2013, **267**, 95-103.
10. R. T. Chacko, J. Ventura, J. Zhuang and S. Thayumanavan, *Adv. Drug Del. Rev.*, 2012, **64**, 836-851.
11. A. Sosnik, J. das Neves and B. Sarmento, *Prog. Polym. Sci.*, 2014, **39**, 2030-2075.
12. S. Vrignaud, J.-P. Benoit and P. Saulnier, *Biomaterials*, 2011, **32**, 8593-8604.
13. K. Kataoka, A. Harada and Y. Nagasaki, *Adv. Drug Del. Rev.*, 2001, **47**, 113-131.
14. P. Tanner, P. Baumann, R. Enea, O. Onaca, C. Palivan and W. Meier, *Acc. Chem. Res.*, 2011, **44**, 1039-1049.
15. D. Peer, J. M. Karp, S. Hong, O. C. FaroKhzad, R. Margalit and R. Langer, *Nat. Nanotechnol.*, 2007, **2**, 751-760.
16. X. Ma and H. Tian, *Acc. Chem. Res.*, 2014, **47**, 1971-1981.
17. A. S. Hoffman, *Adv. Drug Del. Rev.*, 2013, **65**, 10-16.
18. S. Dai, P. Ravi and K. C. Tam, *Soft Matter*, 2008, **4**, 435-449.
19. C. J. F. Rijcken, O. Soga, W. E. Hennink and C. F. van Nostrum, *J. Control. Release*, 2007, **120**, 131-148.
20. F. H. Meng, Z. Y. Zhong and J. Feijen, *Biomacromolecules*, 2009, **10**, 197-209.
21. Z.-Y. Qiao, R. Ji, X.-N. Huang, F.-S. Du, R. Zhang, D.-H. Liang and Z.-C. Li, *Biomacromolecules*, 2013, **14**, 1555-1563.
22. Z.-Y. Qiao, R. Zhang, F. S. Du, D. H. Liang and Z. C. Li, *J. Control. Release*, 2011, **152**, 57-66.
23. Z.-Y. Qiao, F. S. Du, R. Zhang, D. H. Liang and Z. C. Li, *Macromolecules*, 2010, **43**, 6485-6494.
24. Y. Wang, Q. Luo, R. Sun, G. Zha, X. Li, Z. Shen and W. Zhu, *J. Mater. Chem. B*, 2014, **2**, 7612-7619.
25. H. Wang, J. He, M. Zhang, Y. Tao, F. Li, K. C. Tam and P. Ni, *J. Mater. Chem. B*, 2013, **1**, 6596-6607.
26. W. Lin, S. Nie, Q. Zhong, Y. Yang, C. Cai, J. Wang and L. Zhang, *J. Mater. Chem. B*, 2014, **2**, 4008-4020.
27. J. O. Lee, K. T. Oh, D. Kim and E. S. Lee, *J. Mater. Chem. B*, 2014, **2**, 6363-6370.
28. E. S. Lee, J. H. Kim, T. Sim, Y. S. Youn, B.-J. Lee, Y. T. Oh and K. T. Oh, *J. Mater. Chem. B*, 2014, **2**, 1152-1159.
29. D. M. Lynn, M. M. Amiji and R. Langer, *Angew. Chem. Int. Ed.*, 2001, **40**, 1707-1710.
30. J. Ko, K. Park, Y. S. Kim, M. S. Kim, J. K. Han, K. Kim, R. W. Park, I. S. Kim, H. K. Song, D. S. Lee and I. C. Kwon, *J. Control. Release*, 2007, **123**, 109-115.
31. D. Shenoy, S. Little, R. Langer and M. Amiji, *Mol. Pharm.*, 2005, **2**, 357-366.
32. W. Song, Z. Tang, M. Li, S. Lv, H. Yu, L. Ma, X. Zhuang, Y. Huang and X. Chen, *Macromol. Biosci.*, 2012, **12**, 1375-1383.
33. J. Chen, X. Qiu, J. Ouyang, J. Kong, W. Zhong and M. M. Xing, *Biomacromolecules*, 2011, **12**, 3601-3611.
34. Y. Shen, H. Tang, Y. Zhan, E. A. Van Kirk and W. J. Murdoch, *Nanomed. Nanotechnol. Biol. Med.*, 2009, **5**, 192-201.
35. Z.-Y. Qiao, C. Hou, D. Zhang, Y. Liu, Y.-X. Lin, H.-W. An, X.-J. Li and H. Wang, *J. Mater. Chem. B*, 2015, DOI: 10.1039/C1034TB02144D.
36. Z.-Y. Qiao, S.-L. Qiao, G. Fan, Y.-S. Fan, Y. Chen and H. Wang, *Polym. Chem.*, 2014, **5**, 844-853.
37. Z. Duan, Y. Gao, Z.-Y. Qiao, G. Fan, Y. Liu, D. Zhang and H. Wang, *J. Mater. Chem. B*, 2014, **2**, 6271-6282.
38. V. Ozdemir, B. Williams-Jones, S. J. Glatt, M. T. Tsuang, J. B. Lohr and C. Reist, *Nat. Biotechnol.*, 2006, **24**, 942-947.
39. T. Lammers, V. Subr, K. Ulbrich, W. E. Hennink, G. Storm and F. Kiessling, *Nano Today*, 2010, **5**, 197-212.

40. K. H. Bae, H. J. Chung and T. G. Park, *Molecules and Cells*, 2011, **31**, 295-302.

41. J. A. Barreto, W. O'Malley, M. Kubeil, B. Graham, H. Stephan and L. Spiccia, *Adv. Mater.*, 2011, **23**, H18-H40.

42. Y. Cheng, L. Zhao, Y. Li and T. Xu, *Chem. Soc. Rev.*, 2011, **40**, 2673-2703.

43. J. Nam, N. Won, J. Bang, H. Jin, J. Park, S. Jung, S. Jung, Y. Park and S. Kim, *Adv. Drug Del. Rev.*, 2013, **65**, 622-648.

44. X. Ma, Y. Zhao and X.-J. Liang, *Acc. Chem. Res.*, 2011, **44**, 1114-1122.

45. Z. Ge and S. Liu, *Chem. Soc. Rev.*, 2013, **42**, 7289-7325.

46. U. Mayerhoeffer, B. Fimmel and F. Würthner, *Angew. Chem. Int. Ed.*, 2012, **51**, 164-167.

47. J. R. Johnson, N. Fu, E. Arunkumar, W. M. Leevy, S. T. Gammon, D. Piwnica-Worms and B. D. Smith, *Angew. Chem. Int. Ed.*, 2007, **46**, 5528-5531.

48. J. J. Gassensmith, J. M. Baumes and B. D. Smith, *Chem. Commun.*, 2009, 6329-6338.

49. J.-J. Lee, A. G. White, J. M. Baumes and B. D. Smith, *Chem. Commun.*, 2010, **46**, 1068-1069.

50. H. Wang, T. E. Kaiser, S. Uemura and F. Würthner, *Chem. Commun.*, 2008, 1181-1183.

51. T. Heek, F. Würthner and R. Haag, *Chem. Eur. J.*, 2013, **19**, 10911-10921.

52. U. Mayerhoeffer, M. Gsaenger, M. Stolte, B. Fimmel and F. Würthner, *Chem. Eur. J.*, 2013, **19**, 218-232.

53. F. P. Gao, Y. X. Lin, L. L. Li, Y. Liu, U. Mayerhoffer, P. Spenst, J. G. Su, J. Y. Li, F. Wurthner and H. Wang, *Biomaterials*, 2014, **35**, 1004-1014.

54. Y. Liu, L.-L. Li, G.-B. Qi, X.-G. Chen and H. Wang, *Biomaterials*, 2014, **35**, 3406-3415.

55. Y. Liu, F.-P. Gao, D. Zhang, Y.-S. Fan, X.-G. Chen and H. Wang, *J. Control. Release*, 2014, **173**, 140-147.

56. D. Zhang, Y.-X. Zhao, Z.-Y. Qiao, U. Mayerhöffer, P. Spenst, X.-J. Li, F. Würthner and H. Wang, *Bioconjugate Chem.*, 2014, **25**, 2021-2029.

57. Z.-Y. Qiao, J. Cheng, R. Ji, F.-S. Du, D.-H. Liang, S.-P. Ji and Z.-C. Li, *RSC Adv.*, 2013, **3**, 24345-24353.

58. K. Byagari, A. Shanavas, A. K. Rengan, G. C. Kundu and R. Srivastava, *J. Biomed. Nanotechnol.*, 2014, **10**, 109-119.

59. H.-Y. Huang, S.-H. Hu, C.-S. Chian, S.-Y. Chen, H.-Y. Lai and Y.-Y. Chen, *J. Mater. Chem.*, 2012, **22**, 8566-8573.

60. Z. Liu and P. Yao, *Polym. Chem.*, 2014, **5**, 1072-1081.

61. R. Tong, H. D. Hemmati, R. Langer and D. S. Kohane, *J. Am. Chem. Soc.*, 2012, **134**, 8848-8855.

62. A. I. Minchinton and I. F. Tannock, *Nat. Rev. Cancer*, 2006, **6**, 583-592.

The co-encapsulation of RA-V cyclopeptide and SQ molecules in pH-sensitive PAE micelles for efficient tumor therapy and imaging *in vitro* and *in vivo*.